CHAPTER 5

^{1}H NMR Structural Evidence for a Mismatch Specific Intercalator: [Rh(bpy)$_2$chrysi]$^{3+}$ Bound to d(GCCTCAGGC)$_2$

Abstract

^{1}H NMR spectroscopy was employed to study the binding of $[Rh(bpy)_2chrysi]^{3+}$ (chrysi = 5,6-chrysenquinone diimine) to the ninemer oligonucleotide $d(GCCTCAGGC)_2$ which contains a centrally placed CC mismatch. Issues of intercalation and mismatch specificity have been explored. Two forms of evidence support intercalation by the metal complex within the mismatch site (i) upfield chemical shifts and significant broadening of the chrysi resonances and (ii) an increase in duplex melting temperature in the presence of the metal complex. Slow exchange on the NMR timescale is achieved at 5° C, thus permitting the observation of the bound complex. To simplify the NMR spectra and to minimize resonances associated with different competing binding modes, the Δ isomer of $[Rh(d_8\text{-}bpy)_2chrysi]^{3+}$ was employed in the NMR experiments. A break in the connectivity in the NOE walk is observed between T_4 and C_5, thereby marking the binding site of the metal complex at the CC mismatch. Intermolecular NOE's place the metal complex in the major groove of the oligonucleotide. From the combined NMR data, it is concluded that $[Rh(bpy)_2chrysi]^{3+}$ intercalates specifically at the CC mismatch site of the oligonucleotide from the major groove.

Introduction

Since the discovery of small octahedral metal complexes that intercalate into DNA (1), much work has been done to design metallointercalators having sequence specific recognition feature (2). Octahedral rhodium(III) complexes containing the phi ligand bind avidly to double-helical DNA by intercalation (3); on photoactivation, direct DNA strand cleavage is also promoted at the bound site (4). By tuning the ancillary ligands, complexes can be prepared that are either site-specific or sequence-neutral. [Rh(bpy)phi$_2$]$^{3+}$ (bpy, 2,2'-bipyridine), for example, binds to B-DNA with little site selectivity (4), whereas [Rh(*S*,*S*-dimethyltrien)(phi)]$^{3+}$ specifically targets the sequence 5'-TGCA-3' (5). The high-resolution crystal structure of [Rh(*S*,*S*-dimethyltrien)(phi)]$^{3+}$ bound to a DNA octamer shows site-specific intercalation by the complex from the major groove side of the helix, with site-discrimination determined through an ensemble of hydrogen bonding contacts and methyl-methyl interactions (6). The intercalated phi ligand itself resembles another base pair, stacked at a distance of 3.4 Å between neighboring base pairs, with an expanse across the ligand of dimensions matching that of the base pairs above and below.

Recently, targeting single-base mismatches in DNA is becoming a challenging problem in molecular recognition. What distinguishes such a site, instead, is the local destabilization in opposing bases because of the absence of Watson-Crick hydrogen bonding (7). In our laboratory, we have exploited the local helix destabilization associated with mispairing in the design of a metal complex targeted to mismatches (8-10). The chrysene quinone diimine (chrysi) complex, [Rh(bpy)$_2$chrysi]$^{3+}$ (bpy, 2,2'-bipyridine; chrysi, 5,6-chrysenquinone diimine) with sterically expansive chrysi ligand represents such a metal complex targeted to mismatches (8). The site-specificity of the complex is derived from the fact that it is a more bulky intercalator with an expanse

exceeding that of the well matched base pair. Owing to shape selection, the complex is unable to bind to well matched B-form DNA. However, at sites where a base pair is destabilized, intercalation of the chrysi complex can occur with high binding affinity (k_b: 8.4×10^5 M^{-1} for oligonucleotides containing a CC mismatch) (8). $[Rh(bpy)_2chrysi]^{3+}$ has been shown to be both a general and a remarkably specific mismatch recognition agent (11, 12). Specific DNA cleavage is observed at >80% of mismatch sites in all of the possible single base-pair sequence contexts around the mispaired bases. Moreover, the complex was found to recognize and photocleave at a single base mismatch in a 2,725-bp linearized plasmid heteroduplex. Recently, metal complex which targets mismatches, $[Rh(bpy)_2phzi]^{3+}$ (phzi, benzo[a]phenazine-5,6-quinone diimine) has been synthesized (10). This complex shares a sterically demanding intercalating ligand like the chrysi complex and binds to mismatched sites with a higher binding affinity and site-selectivity.

These site-specific mismatch complexes could have promising application in the design of novel chemotherapeutics. They could be used in discovery efforts to identify single-nucleotide polymorphisms. Moreover, many cancers are associated with a deficiency in mismatch repair (13, 14). Hence, by directing small molecules to the accumulated mismatches, a cancer-specific targeting strategy could be envisioned. However, all these experiments will require a substantial understanding of the processes and mechanism of these mismatch targeting agents. Thus to understand how these mismatch-recognizing metal complexes bind site specifically to the mismatches in DNA, it is crucial to obtain structural data on these metal complex-oligonucleotide systems. Here we report an NMR investigation, probing the binding of $[Rh(bpy)_2chrysi]^{3+}$ to a ninemer DNA containing a CC mismatch in a self-complementary duplex, d(GCCTCAGGC)$_2$. These results are important to consider not only in the general

context of intercalator – DNA interactions, but also with respect to the mechanism of mismatch recognizing agents.

Material and Methods

99.96% deuterated D_2O and sodium 3-trimethylsilyl-[2,2,3,3-D_4]propionate (TMSP) were obtained from Aldrich Chemical Co. Other chemicals and biochemicals were of highest quality available commercially. Deuterated (d8) 2,2'-Bipyridine was purchased from Cambridge Isotopes.

Synthesis of [Rh(bpy)$_2$chrysi]Cl$_3$ and [Rh(d$_8$-bpy)$_2$chrysi]Cl$_3$. The metal complexes (bpy = 2,2'-bipyridine; d$_8$-bpy = d_8-2,2'-Bipyridine; chrysi = 5,6-chrysenquinone diimine) were prepared according to the procedure reported in the literature (15). The resolution of enantiomers the racemic mixture was separated as described before (15) under dark room conditions on a long Sephadex CM-C25 ion exchange column eluting with 0.15 M (+)-potassium antimonyl tartrate in water.

Oligonucleotide Synthesis and Purification. The self complementary ninemer oligonucleotide with a central CC mismatch was synthesized using standard phosphoramidite chemistry on an Applied Biosystems 392 DNA synthesizer with a dimethoxy trityl protective group on the 5' end. The oligonucleotide was then purified on a reversed-phase Rainin Dynamax C_{18} column on a Hewlett-Packard 1050 HPLC using 50 mM triethylammonium acetate and an acetonitrile gradient and deprotected by incubation in 80% acetic acid for 15 minutes. After deprotection, the oligonucleotide was purified again by HPLC and desalted in a Waters C_{18} SepPak column and converted to the sodium salt using CM Sephadex C-25 (Sigma) equilibrated in NaCl and washed well with water. The concentration of the oligonucleotide was determined by UV-visible spectroscopy (Beckman DU 7400) using the extinction coefficients estimated for single-stranded DNA: ε(260 nm, $M^{-1}cm^{-1}$) adenine (A) = 15,400; guanine (G) = 11,500; cytosine (C) = 7,400; thymine (T) = 8,700. The duplex was annealed in Perkin Elmer

Cetus Thermal Cycler by gradual cooling from 90 °C to ambient temperature in 90 mins. Duplex formation was evaluated by examining its temperature-dependent absorbance at 260 nm.

Melting Temperature Experiments. The melting temperatures of the duplex and 1:1 duplex + Δ-[Rh(bpy)$_2$chrysi]$^{3+}$ were determined from absorbance versus temperature curves measured at 260 nm on a Beckman DU 7400 UV-visible spectrophotometer. 10 μM duplex was used in a buffer of 5 mM NaCl, 15 mM sodium phosphate, pH 7.0.

Sample Preparation for NMR Analysis and Instrumental Methods. ^{1}H NMR spectra were recorded in Varian Unity*PLUS*-600 spectrometer with variable temperature control and pulsed-field gradients in three dimensions. For the DNA-metal complex titration experiments, the oligonucleotide samples contained 0.9 mM duplex, 5mM NaCl, 15 mM sodium phosphate, pD 7.0 in 100% D$_2$O. The free metal complex sample contained 9 mM of the metal complex in the same buffer. The chemical shifts are related relative to TMSP at 278 K. Samples were repeatedly freeze-dried from D$_2$O and finally made up in 99.96% D$_2$O. One-dimensional NMR and NOESY experiments were carried out at 5 °C. For the titration of metal complex, the initial metal complex solution was taken in acetonitrile at 5 mM. The buffer solution was added to the acetonitrile solution. Spectra recorded in D$_2$O were collected with presaturation of the residual water signal. Typical instrument setting for acquiring one dimensional spectra in D$_2$O at 600 MHz were as follows: sweep width, 6492 Hz; number of scans, 128; relaxation delay, 1.3s; spectral size, 4416 data points with -0.5 Hz line broadening. Two dimensional phase sensitive NOESY spectra were recorded using 2048 points in t$_2$ for 512 t$_1$ values with a mixing time of 125 ms. DQCOSY experiments were accumulated using 2048 data points in t$_2$ for 256 t$_1$ values with a pulse repetition delay of 1.7s. Data were processed and analyzed using the VNMR software (version 6.1b) on a SUN workstation.

Molecular Modeling. The coordinates for the metal complex were taken from the crystal structure (16). The mismatch binding site was constructed using Insight II molecular modeling software while the metal complex was manually docked using the Weblab viewer Pro 3.7

Results

Assignment of the ^{1}H NMR Resonances.

Oligonucleotide: The ^{1}H NMR spectrum of the free d(GCCTCAGGC)$_2$ was assigned by standard techniques (17). In right handed B-DNA duplexes, the base proton (H8 or H6) exhibit NOEs to its own and 5'-flanking sugar H1' and H2'2" protons, allowing an NOE walk from the 5'-to the 3'-end of the oligonucleotide. A clear NOE walk was observed identifying the aromatic and sugar H1' (Figure 4). A point to note that based on the NOE walk, it is likely that the cytosines at the mismatch site are inserted and stacked between the flanking base pairs, rather than being positioned primarily in an extrahelical position. Analysis of short mixing time NOESY spectra and the observation of imino protons from the non-terminal base pairs indicated that the ninemer adopts a right-handed B-form in solution.

Metal complex: The ^{1}H NMR of Δ-[Rh(bpy)$_2$chrysi]$^{3+}$ has been quite complex to assign owing to the abundance of aromatic resonances (Figure 1). To simplify the proton resonances and particularly assign the resonances of the intercalating chrysi moiety, [Rh(d$_8$-bpy)$_2$chrysi]$^{3+}$ was synthesized. However, the ^{1}H NMR of the Δ-Rh(d$_8$-bpy)$_2$chrysi]$^{3+}$ in D$_2$O was difficult to assign as well (Figure 2). The close positioning and overlapping of the five protons of the chrysi ligand made it especially complicated to enable unambiguous resonance assignment. The DQCOSY spectrum of the metal complex in D$_2$O yielded little useful information. Interestingly, the ^{1}H NMR spectra of the metal complex in acetonitrile at 278 K showed clear splitting (six doublets (d) and
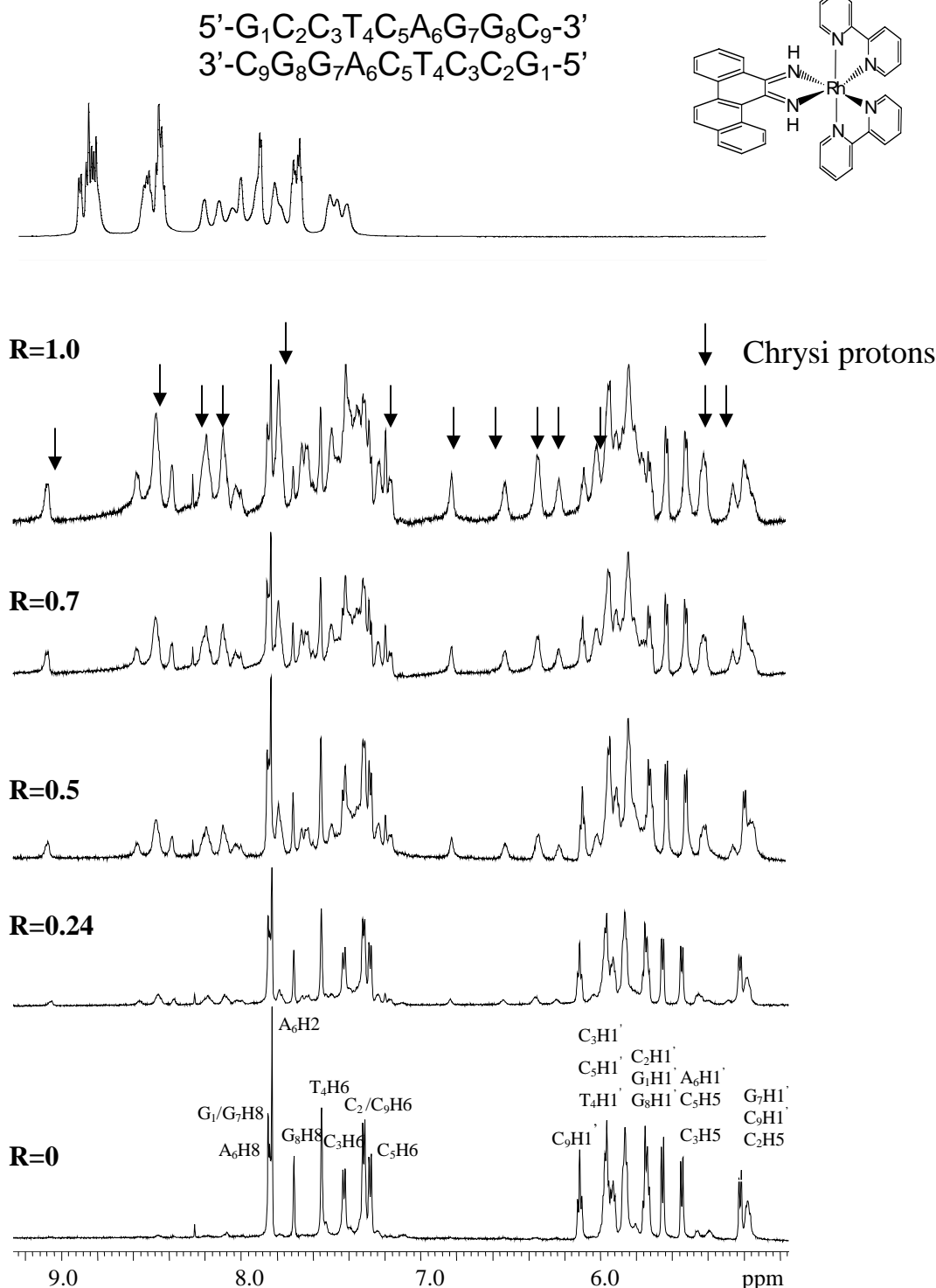
5'-$G_1C_2C_3T_4C_5A_6G_7G_8C_9$-3'
3'-$C_9G_8G_7A_6C_5T_4C_3C_2G_1$-5'

Figure 5.1. 600 MHz (Varian INOVA) one dimensional ^{1}H NMR spectra of Δ-[Rh(bpy)$_2$chrysi]$^{3+}$ titrated into d($G_1C_2C_3T_4C_5A_6G_7G_8C_9$)$_2$, at 278K : R (metal:duplex ratios) = 0, 0.24, 0.5, 0.7 and 1. Shown is the aromatic and sugar H$_1$' region. The oligonucleotide has been assigned using 2D NOESY experiments. Due to overlapping peak positions, it is not possible to assign the resonances for the chrysi ligand. The upfield shifted chrysi resonances are marked with arrows. The oligonucleotide and [Rh(bpy)$_2$chrysi]$^{3+}$ were prepared as previously described. The DNA samples contained 0.9 mM duplex, 5mM NaCl, 15 mM sodium phosphate, pD 7.0 in 100% D$_2$O. The free metal complex sample contained 9 mM Δ-[Rh(bpy)$_2$chrysi]$^{3+}$ in the same buffer. The chemical shifts are related relative to TMSP at 278 K.
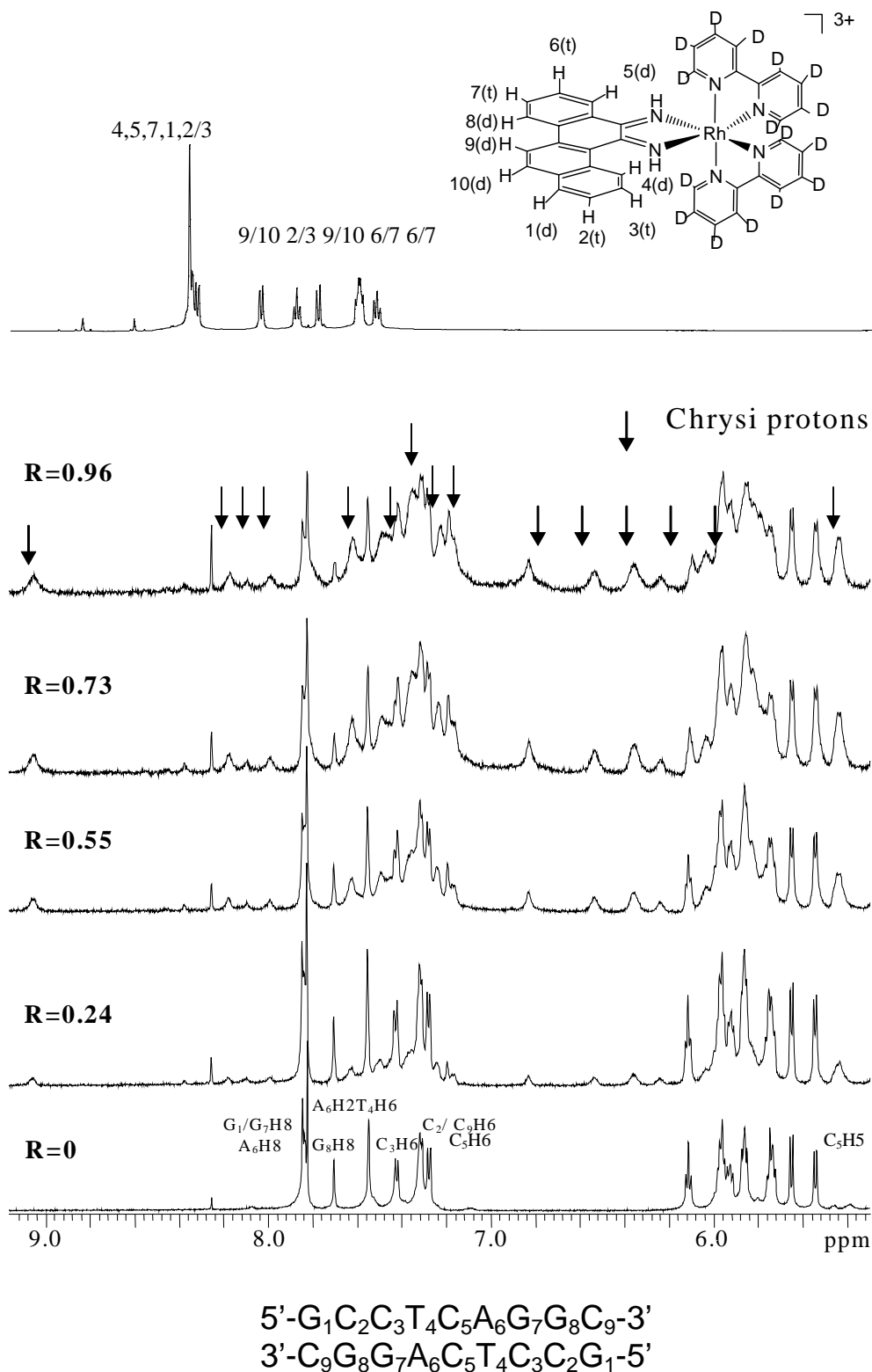
Figure 5.2. 600 MHz (Varian INOVA) one dimensional ^{1}H NMR spectra of Δ-[Rh(d$_8$-bpy)$_2$chrysi]$^{3+}$ titrated into d(G$_1$C$_2$C$_3$T$_4$C$_5$A$_6$G$_7$G$_8$C$_9$)$_2$, at 278K : R (metal:duplex ratios) = 0, 0.24, 0.55, 0.73 and 0.96. Shown is the aromatic and sugar H$_1$' region. The upfield shifted chrysi resonances are marked with arrows. The DNA samples contained 0.9 mM duplex, 5mM NaCl, 15 mM sodium phosphate, pD 7.0 in 100% D$_2$O. The free metal complex sample contained 9 mM Δ-[Rh(d$_8$-bpy)$_2$chrysi]$^{3+}$ in the same buffer. The chemical shifts are related relative to TMSP at 278 K.

4d, 1d, 8d, 2/3t ,5d   9/10d   2/3t 9/10d 6/7t 6/7t

V= 29%

V= 16%

V= 7%

V= 4%

V= 2%

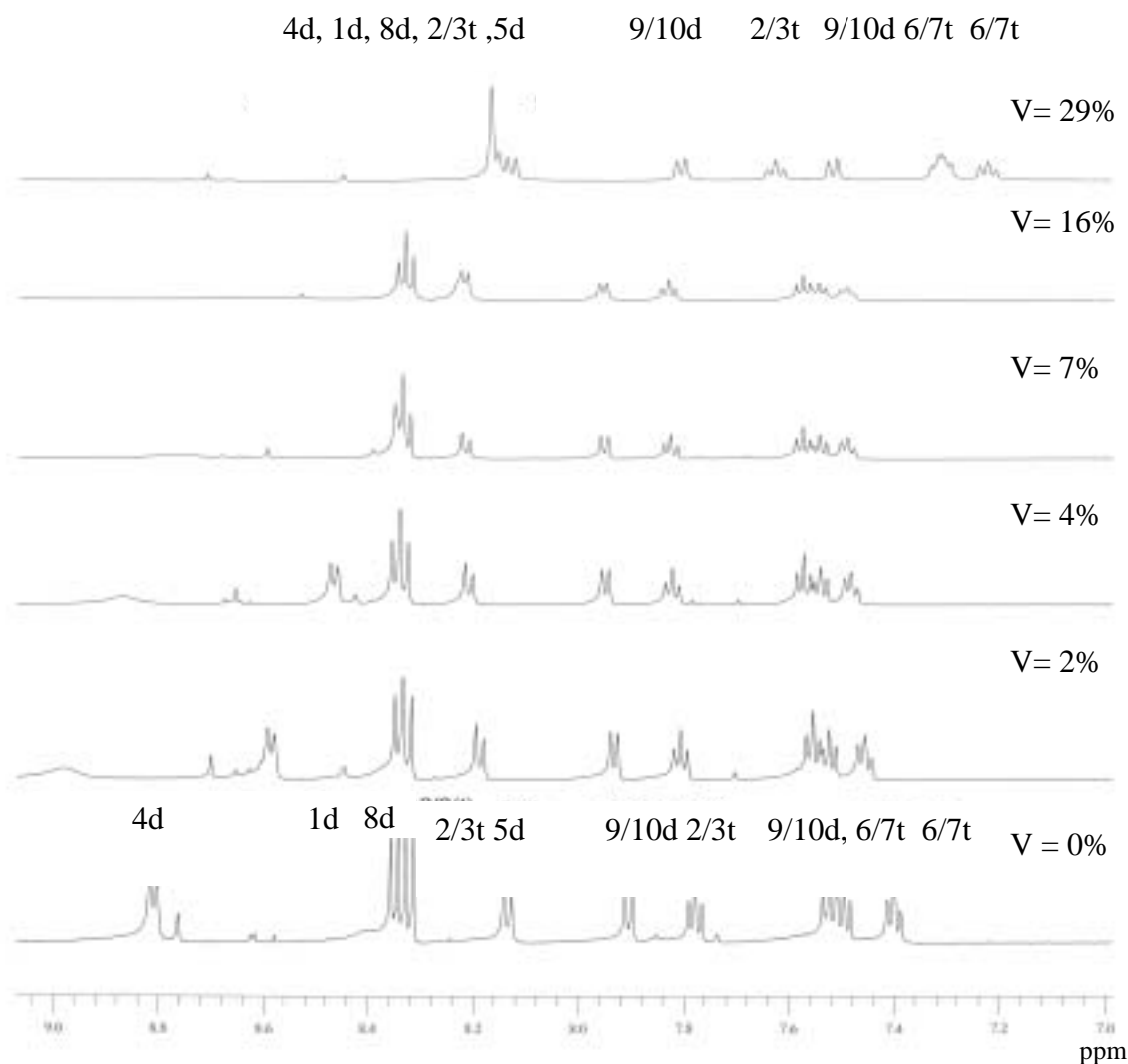4d   1d   8d   2/3t 5d   9/10d 2/3t   9/10d, 6/7t   6/7t   V = 0%

ppm

Figure 5.3.   600 MHz (Varian INOVA) one dimensional ^{1}H NMR spectra of buffered D_2O titrated into an acetonitrile solution of Δ-[Rh(d$_8$-bpy)$_2$chrysi]$^{3+}$ at 278K : V (Volume percentage of D_2O wrt acetonitrile) = 0, 2, 4, 7, 16 and 29. Buffer stock solution: 5 mM NaCl, 15 mM sodium phosphate, pD 7.0 in 100% D_2O. The metal complex sample contained 9 mM of Δ-[Rh(d$_8$-bpy)$_2$chrysi]$^{3+}$ in acetonitrile. The chemical shifts are related relative to TMSP at 278 K. (d) and (t) refers to doublet and triplet peak splitting respectively.

four triplets(t)) and all the ten protons from the Δ-Rh(d$_8$-bpy)$_2$chrysi]$^{3+}$ were well

resolved (Figure 3). It is however crucial to establish the proton resonances of the metal

complex in aqueous medium to reach meaningful interpretations. To map the proton

resonances of the metal complex under the two different solvent conditions, a titration

experiment was performed where buffered D$_2$O (5mM NaCl, 15 mM sodium phosphate,

pD 7.0) was increasingly added to a solution of the Δ-Rh(d$_8$-bpy)$_2$chrysi]$^{3+}$ in acetonitrile

and the shifts of the different metal complex resonances were followed (Figure 3). When

the percentage volume of D$_2$O is 29, the NMR spectrum of the metal complex looked

identical to that previously recorded in D$_2$O (Figure 2) and titration was discontinued.

The DQCOSY spectrum of the metal complex in acetonitrile provided the connectivity

relationship among the protons attached to three different ring systems, however the

DQCOSY spectrum did not reveal the identity of the protons in the ^{1}H NMR spectra. To

assign the proton resonances of the chrysi ligand in Δ-Rh(d$_8$-bpy)$_2$chrysi]$^{3+}$, we relied on

observation of the titration data coupled with our knowledge about the structure of the

metal complex.

On addition of D$_2$O to the acetonitrile solution of the metal complex, the proton

resonances move upfield in general (Figure 3). However, the shifts of two protons

(assigned as 4(d) and 5(d)) are considerably more compared to the rest. Particularly, the

proton assigned as 4(d) moved sharply upfield on the addition of D$_2$O. The resonance

assigned as 5(d) moved little downfield while merging with the large collection of

resonances (1(d), 8(d), 2/3(t)) moving upfield. The X-ray structure (16) of the metal

complex revealed short interatomic distance between the 4(d) and the imine (–NH)

protons which points to strong steric clashes between the two protons. 5(d) proton also

experiences some steric strain with its corresponding imine proton, however to a lesser

extent than that of 4(d). 5(d) proton forms a hypothetical six membered ring with its

neighboring imine proton while the 4(d) forms a more strained five membered ring

system. This is also reflected in the differential acidity of the two imine protons of the chrysi moiety in the metal complex. Once the 4(d) and 5(d) protons are assigned, it becomes relatively straightforward to identify the rest of the proton resonances by following the connectivity of the ring systems as obtained from DQCOSY spectrum. The assignment of the ^{1}H NMR spectrum of Δ-Rh(d$_8$-bpy)$_2$chrysi]$^{3+}$ in water is finally obtained by following shifts of the assigned proton resonances of the metal complex in acetonitrile. The imine proton resonances of the chrysi complex are not evident as a result of their high acidity.

Δ-Rh(bpy)$_2$chrysi]$^{3+}$ + d(GCCTCAGGC)$_2$ Binding Studies: The NMR spectrum of d(GCCTCAGGC)$_2$ with added Δ-Rh(bpy)$_2$chrysi]$^{3+}$ is shown in Figure 1 together with the spectra of the free metal complex and the ninemer duplex. On addition of the metal complex, only one set of shifted resonances grows in. There is little or no shift in the oligonucleotide proton resonances. This behavior indicates a single bound state and is consistent with the binding of the metal complex at the central CC mismatch of the duplex. The C_2 symmetry of the self-complementary duplex appears to be maintained in the bound form. Slow exchange is achieved for most of the resonances at 278 K. This exchange time is slower than the one observed for Δ-[Rh(phen)$_2$phi]$^{3+}$ (phi= 9,10-phenanthrolinequinone diimine)(3) and must be attributed to the different stacking of the base pairs imparted by the extended chrysi ligand. Dramatic effects on the chemical shifts of the rhodium chrysi complex were observed on binding to DNA; significant upfield shift and broadening of the metal complex protons was observed. Also there are appearances of bound metal complex protons in the relatively uncluttered region (6.1- 7.2 ppm) of the oligonucleotide spectrum.

Δ-Rh(d$_8$-bpy)$_2$chrysi]$^{3+}$ + d(GCCTCAGGC)$_2$: Binding Studies By One Dimensional NMR: To simplify the titration experiment, partially deuterated metal complex was employed (Figure 2). Comparison with the earlier titration spectra (Δ-Rh(bpy)$_2$chrysi]$^{3+}$ + d(GCCTCAGGC)$_2$) revealed that the protons of the chrysi ligands undergo a significant upfield shift (0.1 – 1.5 ppm) upon addition of the metal complex, while the ancillary bipyridyl protons are little or not shifted at all. These shifts are consistent with the preferential partial intercalation of the chrysi ligands at the mismatch site of the DNA duplex (3, 18). The shifts of the chrysi protons upon binding to the oligonucleotide were quantified and are shown in Table 1.

Melting Temperature Studies: DNA binding by intercalation is also generally characterized by an increase in the melting temperature of the DNA (19). The melting temperature (*Tm*) of the free oligonucleotide with central CC mismatch was determined to be 23.7 °C. Addition of stoichiometric Δ-Rh(bpy)$_2$chrysi]$^{3+}$ increased the melting temperature of the duplex by 7 °C, consistent with intercalation (18, 19).

Δ-Rh(d$_8$-bpy)$_2$chrysi]$^{3+}$ + d(GCCTCAGGC)$_2$: Binding Studies By Two Dimensional NMR: NOESY spectra of the oligonucleotide with the added metal complex were recorded at 278 K using mixing times ranging from 100 to 300 ms, to obtain a detailed picture of the metal complex binding. The NOESY data at 125 ms show the clearest cross peak contours. In the diagnostic base – sugar H2'H2" region of the NOESY spectra, a distinct break is observed in the sequential connectivities at the central 5'-C$_5$A$_6$-3'. This suggests site-specific intercalation of the metal complex at the CC mismatch of the duplex even at millimolar concentration (Figure 4). Thus this result provides direct evidence, consistent with photocleavage study (10), for intercalation at this specific base step.

NOESY spectra yield distinct intermolecular NOE's between chrysi protons and the oligonucleotide protons in the region of intercalation (Figure 5). Strong evidence for

the success of the design of this complex comes from the detection of the intermolecular NOE's between the 6(t) and 7(t) protons of the chrysi ligand and the two aromatic protons of the cytosine bases at the mismatch site. Note that 6(t) and 7(t) chrysi protons are a part of the lateral ring of the chrysi moiety. Evidences for a deep intercalation are supported by the fact that both aromatic cytosine protons make NOEs to different protons of the chrysi ligands. Intermolecular NOEs between the chrysi ligand and T2CH3 and sugar H2'/H2" protons has also been observed. The observation of all these NOEs with major groove protons points to the fact that the rigid complex intercalates from the major groove. It is noteworthy that the only minor groove aromatic proton A_6H2 shows no crosspeak with the intercalated chrysi protons and remains sharp even at 1:1 ratio of metal and duplex.

A DQCOSY experiment was also employed to assign the bound protons of the chrysi ligand (Figure 6). The 9,10 protons of the chrysi ligand are not a part of through-bond coupled system and therefore are easily identified by DQCOSY. However, they are not the ones which are moved upfield in the relatively uncluttered region of the spectra. Therefore, the 9,10 chrysi protons do not seem to be involved in intercalation which implies that the lateral rings of the chrysi ligand are primarily involved in the intercalating process.

Table 5.1. ^{1}H NMR Chemical Shift^a Changes in Δ-[Rh(d$_8$-bpy)$_2$chrysi]$^{3+}$ upon Binding to DNA

protons of chrysi ligand^b	in D$_2$O buffer^{c,d} δ$_{free}$(ppm)	in 1:1 complex with d(GCCTCAGGC)$_2$^{c,d} δ$_{bound}$ (ppm)	change in shift upon binding Δδ(ppm)
1(d)	8.35	(8.37, 8.56, 8.66)	-----
2,3(t)	8.35, 7.90	8.29,7.68	-0.06, -0.22
4(d)	8.35	(8.37, 8.56, 8.66)	-----
5(d)	8.32	8.18	-0.14
6,7 (t)	7.63, 7.56	7.41,7.38	-0.22, -0.18.
8(d)	8.35	(8.37, 8.56, 8.66)	-----
9,10 (d)	8.05, 7.81	7.82,7.68	-0.23, -0.13

^{a}All spectra were recorded at 600 MHz on Varian *INOVA*. ^{b} The labeling scheme for the complex is indicated in Figure 2. Also given within the parentheses is the splitting of the proton resonances. ^{c}The chemical shifts are related relative to TMSP (±0.02 ppm) at 278 K. ^{d}The DNA samples contained 0.9 mM duplex, 5mM NaCl, 15 mM sodium phosphate, pD (uncorrected) 7.0 in 100% D$_2$O. The free metal complex sample contained 9 mM Δ-[Rh(d$_8$-bpy)$_2$chrysi]$^{3+}$ in the same buffer.

Figure 5.4. Two dimensional ^{1}H NMR spectra of the free duplex d(GCCTCAGGC)$_2$ and Δ-[Rh(d$_8$-bpy)$_2$chrysi]$^{3+}$ bound to d(GCCTCAGGC)$_2$ in 1:1 ratio. Shown are two contour plots of the aromatic – sugar H2'H2" regions of 125 ms NOESY spectra at 278K of the free DNA duplex and 1:1 Δ-[Rh(d$_8$-bpy)$_2$chrysi]$^{3+}$ - d(GCCTCAGGC)$_2$. The lines illustrate the NOE walk along the oligonucleotide. Note the loss of intensity at the 5'-CA-3' step. The DNA samples contained 0.9 mM duplex, 5mM NaCl, 15 mM sodium phosphate, pD 7.0 in 100% D$_2$O. The free metal complex sample contained 9 mM Δ-[Rh(bpy)$_2$chrysi]$^{3+}$ in the same buffer. The chemical shifts are related relative to TMSP at 278 K.
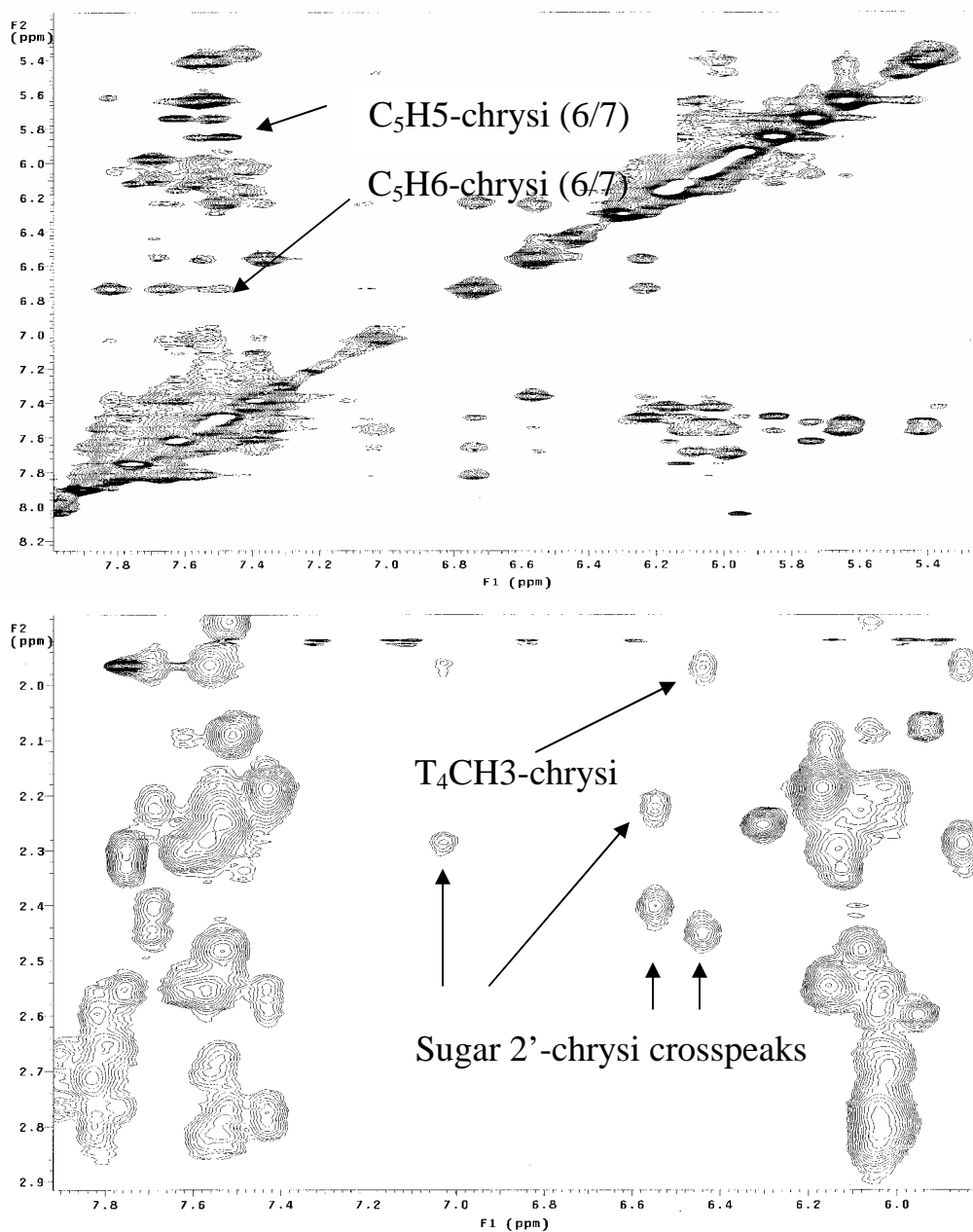
Figure 5.5. Two dimensional ^{1}H NMR spectra of Δ-[Rh(d$_8$-bpy)$_2$chrysi]$^{3+}$ bound to d(GCCTCAGGC)$_2$ in 1:1 ratio at 125 ms mixing time and 278 K. Shown are two contour plots highlighting the intermolecular NOEs between the oligonucleotide and chrysi protons.
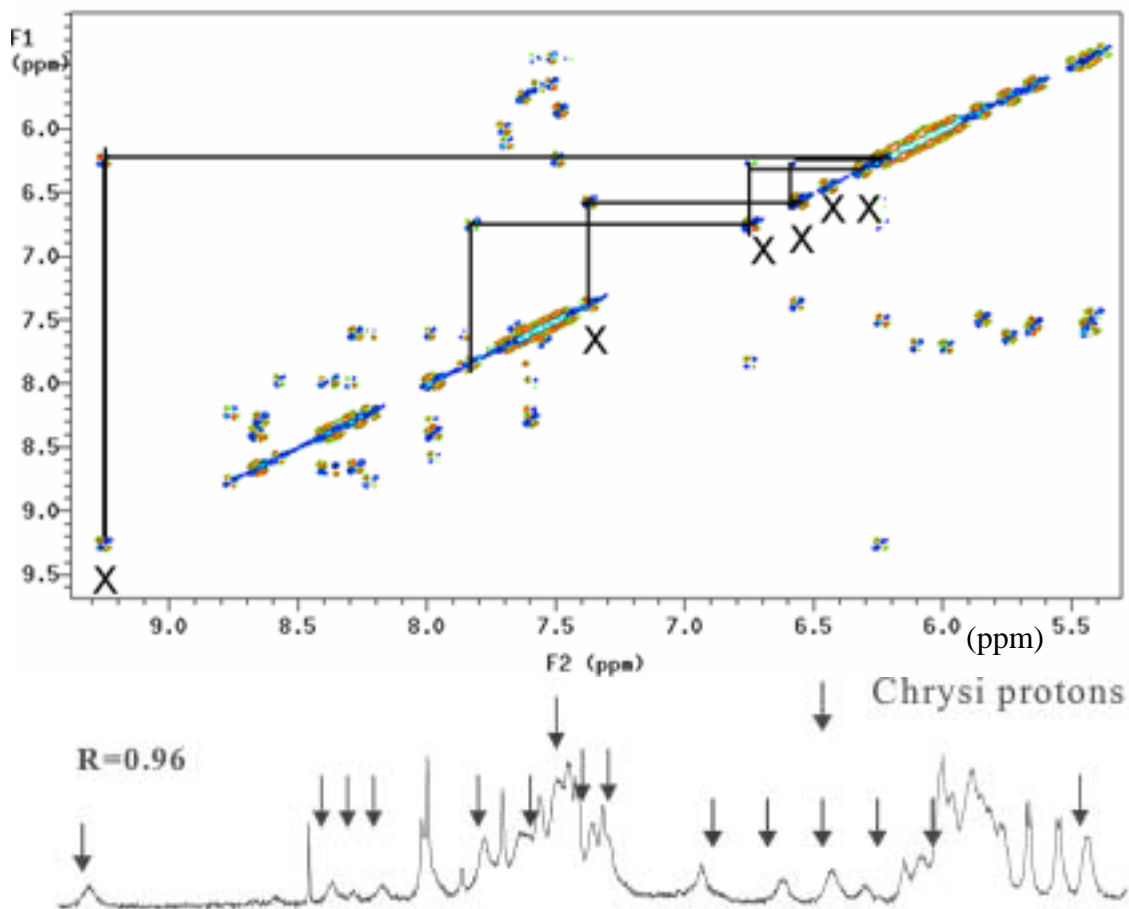
Figure 5.6. DQCOSY spectra of Δ-[Rh(d$_8$-bpy)$_2$chrysi]$^{3+}$ bound to d(GCCTCAGGC)$_2$ in 1:1 ratio. Shown are the contour plot of the aromatic – aromatic region of the DQCOSY spectra at 278K of the free DNA duplex and 1:1 Δ-[Rh(d$_8$-bpy)$_2$chrysi]$^{3+}$ - d(GCCTCAGGC)$_2$. The lines illustrate the connectivity among the chrysi protons in the ligand system . The DNA samples contained 0.9 mM duplex, 5mM NaCl, 15 mM sodium phosphate, pD 7.0 in 100% D$_2$O. The free metal complex sample contained 9 mM Δ-[Rh(d$_8$-bpy)$_2$chrysi]$^{3+}$ in the same buffer. The chemical shifts are related relative to TMSP at 278 K.

Discussions

From the results of ^{1}H NMR studies of Δ-Rh(d$_8$-bpy)$_2$chrysi]$^{3+}$ bound to the CC mismatch site of the self-complementary ninemer duplex, we can draw three main conclusions.

a) The metal complex clearly targets the CC mismatch site. The metal complex binds in such a way that the C_2 symmetry of the system is preserved. There is little or no shift in the oligonucleotide resonances.

b) The binding at the CC mismatch is intercalative. This is supported by the melting temperature studies, the presence of the cross-peaks between the chrysi and C$_5$H5/C$_5$H6 aromatic protons and the break in the connectivity between C$_5$ and A$_6$ bases (Figure 4). The chrysi ligand probably intercalates at the mismatch site pushing the cytosine bases partially towards the phosphodiester backbone to accommodate the bulky intercalating ligand. This is in accordance with the fact that only one disruption in the 5'-C$_5$A$_6$-3' connectivity occurs, while the 5'-T$_4$C$_5$-3' connectivity remains intact.

c) The metal complex intercalates from the major groove of the duplex. The presence of the cross peaks between the C$_5$H5 and C$_5$H6 protons (which are located at the major groove) and the chrysi lateral ring and that of T$_4$CH3 and chrysi proton (Figure 5), unambiguously shows that the intercalation is from the major groove and is consistent with the general observation of other octahedral metal complexes (3, 6, 18, 19).

Figure 7 illustrates a model based upon these data. However, there are certain points which our experiments are unable to address at this stage. Due to the dearth of intermolecular NOEs, it is difficult to develop a model depicting the binding of the metal complex to the mismatch site of the duplex. Furthermore it is not clear how the cytosines at the CC mismatch site are oriented with intercalation of the chrysi moiety. From the

data, it is also not possible to conclude whether the cytosines are extrahelical or intrahelical on binding of the metal complex. However, in the free duplex, the cytosines do appear to be well inserted.

From the limited NMR data, we can conclude that the intercalation of the chrysi is more "side on" than "head on". The NOESY and DQCOSY data both support the idea of intercalation of the chrysi ligand from the side which contains the 6(t) and 7(t) proton. It must be emphasized, however, that we may be looking at only one of the many binding modes of the metal complex to DNA. It is difficult to conceive how C_2 symmetry of the system will be preserved on assuming a lateral intercalation. Moreover, it will be of interest to rationalize why lateral intercalation is favored in one ring over the other. It is also not clear why the intercalation specifically takes place between C_5 and A_6; not between T_4 and C_5. Even though the cross peaks are obtained between C_5 aromatic and chrysi protons; no such cross peaks are observed between A_6 aromatic and chrysi protons. Obviously, more NMR data are required to build up a viable model. X-ray crystallography may also provide an alternative method to obtain structural information about the site-specific binding of the metal complexes at the mismatch site. A cartoon of the metal complex intercalating site specifically at the site of CC mismatch from the major groove of the oligonucleotide is shown in Figure 7. In order to preserve the C_2 symmetry, the two mismatched cytosines (shown in red) at the CC mismatch site unwinds accommodating the chrysi ligand in a stacked fashion.

Conclusions

We report here, NMR structural characterization of a metallointercalator bound site specifically to the mismatch site of a DNA duplex through the intercalation of its bulky ligand. We observe intercalative binding from the major groove of the duplex specifically at the mismatch site. The results demonstrate that shape selectivity of ligand

provides a sensible strategy for the rational construction of site-specific DNA-binding molecules.
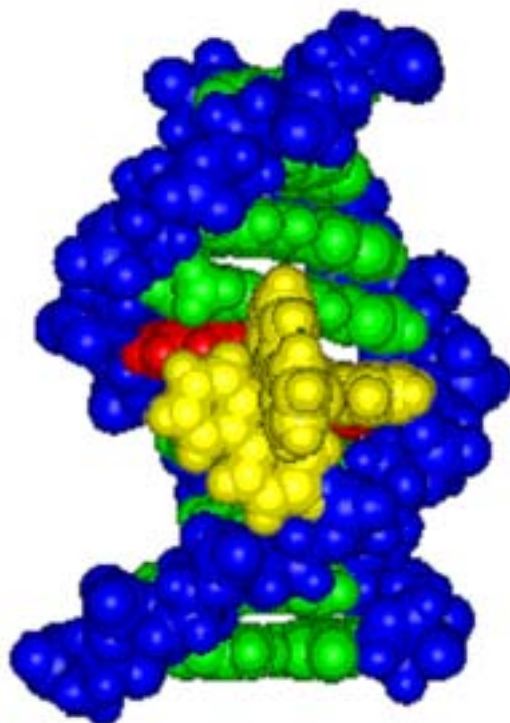
Figure 5.7. Schematic representation of Δ-[Rh(bpy)$_2$chrysi]$^{3+}$ bound to the CC mismatch site of the duplex, d(GCCTCAGGC)$_2$. Shown is the front view of the modeled structure.

References

1   Barton, J. K. (1986) *Science 233*, 727.

2. Erkkila, K. E., Odom, D. T., and Barton, J. K. (1999) *Chem. Rev. 99,* 2777.

3. David, S. S., and Barton, J. K. (1993) *J. Am. Chem. Soc. 115*, 2984.

4. Sitlani, A., Long, E. C., Pyle, A. M., and Barton**,** J. K. (1992) *J. Am. Chem. Soc. 114*, 2303.

5. Krotz, A. H., Hudson, B. P., and Barton, J. K. (1993) *J. Am. Chem. Soc. 115,* 12577.

6. Kielkopf, C. L., Erkilla, K. E., Hudson, B. P., Barton, J. K., and Rees, D. C. (2000) *Nat. Struct. Biol. 7,* 117.

7. Peyret, N., Seneviratne, A., Allawi, H. T., and SantaLucia, J., Jr. (1999) *Biochemistry 28*, 3468.

8. Jackson, B. A., and Barton, J. K. (1997) *J. Am. Chem. Soc. 119*, 12986.

9. Boon, E. M., Kisko, J. L., and Barton, J. K. (2002) *Methods Enzymol. 353*, 506.

10. Junicke, H., Hart, J. J., Kisko, J., Glebov, O., Kirsch, I. R., and Barton, J.K. (2003) *Proc. Nat. Acad. Sci 100*, 3737.

11. Jackson, B. A., Alekseyev, V. Y., and Barton, J. K. (1999) *Biochemistry 38*, 4655.

12. Jackson, B. A., and Barton, J. K. (2000) *Biochemistry 39*, 6176.

13. Duval, A., and Hamelin, R. (2002) *Cancer Res. 62*, 2447.

14. Jacob, S., and Praz, F. (2002) *Biochimie 84*, 27.

15. Murner, H.., Jackson, B. A., and Barton, J. K. (1998**)** *Inorg. Chem. 37*, 3007.

16. Patel, D. J., Shapiro, L., and Hare, D. (1986) *J. Biol. Chem. 261*, 122.

17. Hudson, B. P., Dupureur, C. M., and Barton, J. K. (1995) *J. Am. Chem. Soc. 117,* 9379.

18. Dupureur, C.M., and Barton, J.K. (1998) *Inorg. Chem. 36,* 33.